Inorg. Chem. **1985**, *24*, 1483–1488

Contribution from the Laboratorium für Anorganische Chemie, ETH Zentrum, CH-8092 Zürich, Switzerland, and Istituto di Chimica Farmaceutica, Università di Milano, I-20131 Milano, Italy

Some New Rhodium(I)–Iridium(III) Complexes with Bridging Hydride and Chloride Ligands. Synthesis of Compounds $[L_2Rh(\mu\text{-}H)(\mu\text{-}Cl)IrH_2L'_2]$ ($L = PEt_3$ or L_2 = diphos; $L' = PEt_3$, $P\text{-}i\text{-}Pr_3$) and the X-ray Crystal Structure of $[(PEt_3)_2Rh(\mu\text{-}H)(\mu\text{-}Cl)IrH_2(PEt_3)_2]$

ALBERTO ALBINATI,[1a] HANS LEHNER,[1b] and LUIGI M. VENANZI*[1b]

Received June 18, 1984

The reaction of $[IrH_5(PEt_3)_2]$ with complexes containing the unit "$RhClL_2$" ($L = PEt_3$ or L_2 = diphos, $Ph_2PCH_2CH_2PPh_2$) give compounds $[L_2Rh(\mu\text{-}H)(\mu\text{-}Cl)IrH_2(PEt_3)_2]$. The molecular structure of **8a** ($L = PEt_3$) was determined by X-ray diffraction: monoclinic, space group $P2_1/c$, $Z = 4$, $a = 11.507$ (2) Å, $b = 15.974$ (4) Å, $c = 19.198$ (4) Å, $\beta = 103.19$ (4)°. The structure was solved by Patterson and Fourier methods using 4946 observed reflections ($I \geq 3\sigma(I)$) and refined to a conventional $R = 0.059$. The coordination around rhodium is distorted square planar, and that around iridium is distorted octahedral. The Rh–Ir distance is 2.898 (1) Å, and the bridging chlorine atom is asymmetrically bonded to the two metals. The structural features of this complex are compared with those of a series of related mono- and binuclear complexes. The formation of the dichloro-bridged complex $[(diphos)Rh(\mu\text{-}Cl)_2IrH_2(P\text{-}i\text{-}Pr_3)_2]$ is also reported.

Introduction

Binuclear transition-metal complexes with bridging halide ligands of the type $[L_mM(\mu\text{-}X)_xM'L'_n]$ (x = 1–3) (A) are easily formed.[2] Numerous complexes of the type $[L_mM(\mu\text{-}H)_yM'L'_n]$ (y = 1–4) (B) are also known.[3] Furthermore, in many cases, it is possible to obtain complexes containing both hydride and halide bridging ligands of the type $[L_mM(\mu\text{-}H)_x(\mu\text{-}X)_yM'L'_n]$ ($x + y$ = 2, 3) (C).[3]

While the electronic structure of the bridging unit M–X–M′ in compounds of type A can be described as consisting of two two-electron donor bonds from the halide ion to each of the metal centers,[4,5] that of the M–H–M′ units in compounds of type B requires the postulation of *three-center–two-electron* interactions for each bridging unit.[5–7] Such considerations do not take into account direct M–M′ interactions, which are likely to be more significant in the hydrido- than in the halido-bridged complexes because of the shorter M–M separations in the former class of compounds.

Compounds of type C are of particular interest because they provide an opportunity to study the factors influencing the relative stabilities of μ-H vs. μ-Cl units in bimetallic complexes, e.g., between the different structural types

$$L_mM(\mu\text{-}H)_2M'X_2L'_n \text{ vs.}$$
$$L_mM(\mu\text{-}H)(\mu\text{-}X)M'HXL'_n \text{ vs. } L_mM(\mu\text{-}X)_2M'H_2L'_n$$

It is found that, in some cases, the formation of a three-center–two-electron hydride bridge is preferred over the use of the, at least potentially, two-center–four-electron halide bridge.

It is noteworthy that within a homologous series $[L_mM(\mu\text{-}H)_x(\mu\text{-}X)_yML_m]$ ($x + y$ = 2, 3) marked reactivity differences are observed; e.g., the activity toward catalytic hydrogenation in complexes $[(\eta^5\text{-}C_5Me_5)Rh(\mu\text{-}H)_x(\mu\text{-}Cl)_{3-x}Rh(\eta^5\text{-}C_5Me_5)]^+$ decreases with increasing x.[8] Interesting structural differences for this set of compounds have also been reported.[9]

In a previous publication[10] some of us reported synthetic and structural studies of complexes $[(diphos)Rh(\mu\text{-}H)(\mu\text{-}Cl)IrCl(PEt_3)_3]^+$ (**1a**) and $[(diphos)Rh(\mu\text{-}H)(\mu\text{-}Cl)IrH(PEt_3)_3]^+$ (**2**). We report here an extension of this investigation coupled with a general discussion of the major structural changes in a set of related compounds containing rhodium(I) and iridium(III), as bridged hydride ligands are replaced by halides. The factors determining the preferential formation of hydride vs. chloride bridges will also be discussed.

Results and Discussion

The reaction of $[IrH_5(PEt_3)_2]$[11] (**3a**) with $[(diphos)Rh(\mu\text{-}Cl)_2Rh(diphos)]$[12] (**4**) (diphos = $Ph_2PCH_2CH_2PPh_2$), or its precursor $[RhCl(C_2H_4)(diphos)]$[12] (**5**) (obtained in situ from $[(C_2H_4)_3Rh(\mu\text{-}Cl)_2Rh(C_2H_4)_2]$[13] (**6**) and diphos), gives $[(diphos)Rh(\mu\text{-}H)(\mu\text{-}Cl)IrH_2(PEt_3)_2]$ (**7a**). The related compound $[(PEt_3)_2Rh(\mu\text{-}H)(\mu\text{-}Cl)IrH_2(PEt_3)_2]$ (**8a**) is obtained by the direct reaction of **6**, PEt_3, and **3a**.

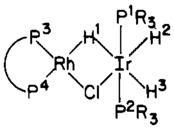

7a, R=Et
b, R=*i*-Pr3
(P⌒P=diphos)

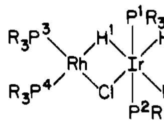

8a, R=Et
b, R=*i*-Pr3

It is noteworthy that the reaction of **6**, diphos, and $IrH_5(p\text{-}i\text{-}Pr_3)_2$[14] (**3b**) failed to give the complex corresponding to **8a**, i.e., $[(diphos)(Rh(\mu\text{-}H)(\mu\text{-}Cl)IrH_2(p\text{-}i\text{-}Pr_3)_2]$ (**8b**). However, impure samples of **8b** were obtained by bubbling H_2 through the reaction mixture. One of the byproducts of this reaction could be isolated and proved to be $[(diphos)Rh(\mu\text{-}Cl)_2IrH_2(p\text{-}i\text{-}Pr_3)_2]$ (**9**).

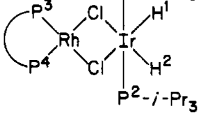

9 (P⌒P=diphos)

---

[1] (a) Università di Milano. (b) ETH Zürich.

[2] Cotton, S. A.; Hart, F. A. "Heavy Transition Elements"; Wiley: New York, 1975.

[3] Venanzi, L. M. *Coord. Chem. Rev.* **1982**, 43, 251 and references quoted therein.

[4] Summerville, R. H.; Hoffmann, R. J. *J. Am. Chem. Soc.* **1979**, *101*, 3821.

[5] Shaik, A.; Hoffmann, R.; Fisel, R.; Summerville, R. H. *J. Am. Chem. Soc.* **1980**, *102*, 4555.

[6] Bau, R.; Teller, R. G.; Kirtley, S. W.; Koetzle, T. F. *Acc. Chem. Res.* **1979**, *12*, 176.

[7] Mason, R.; Mingos, D. P. M. *J. Organomet. Chem.* **1973**, *50*, 53.

[8] Maitlis, P. M. *Acc. Chem. Res.* **1978**, *11*, 301 and references quoted therein.

[9] Churchill, M. R. "Transition Metal Hydrides"; Bau, R., Ed.; American Chemical Society: Washington, DC, 1978; *Adv. Chem. Series No.* 167, p 36.

[10] Lehner, H.; Matt, D.; Togni, A.; Thouvenot, R.; Venanzi, L. M.; Albinati, A. *Inorg. Chem.* **1984**, *23*, 4254.

[11] Chatt, J.; Coffey, R. S.; Shaw, B. L. *J. Chem. Soc.* **1965**, *3791*.

[12] Albano, P.; Aresta, M.; Manassero, M. *Inorg. Chem.* **1980**, *19*, 1069.

[13] Cramer, R. *Inorg. Chem.* **1962**, *1*, 722.

[14] Boron, P.; Musco, A.; Venanzi, L. M. *Inorg. Chem.* **1982**, *21*, 4192 and references quoted therein.

Table I. ^1H NMR Data of the Hydride Ligands in Compounds 7-9

compd	chem shifts, ppm			coupling constants, Hz			
	$\delta(H^1)$	$\delta(H^2)$	$\delta(H^3)$	$^2J(H^1,P^4)$	$^2J(H^1,H^2)$	$^2J(H^3,H^1)$	$^2J(H^2,H^3)$
7a[b]	−12.2	−24.2	−12.7	61	2	16	7
7b[a]	−13.0	−25.6	−14.4	72	2	16	8
8a[a]	−15.1	−23.9	−13.4	64	2	16	7
9[a]		−24.8					

[a] Measured in benzene-d_6. [b] Measured in toluene-d_8.

Table II. ^{31}P NMR Data of Compounds 7-9

compd	chem shifts, ppm			coupling constants, Hz			
	$\delta(P^1)$	$\delta(P^3)$	$\delta(P^4)$	$^1J(Rh,P^3)$	$^1J(Rh,P^4)$	$^2J(P^3,P^4)$	$^4J(P^4,P^1)$
7a[b]	4.2	80.0	58.8	202.5	172.8	35.3	3.3
7b[b]	37.8	78.0	56.6	206.0	168.0	35.0	2.9
8a[a]	4.0	34.9	18.9	198.6	169.1	42.7	2.9
9[a]	33.4	75.9		194.0			

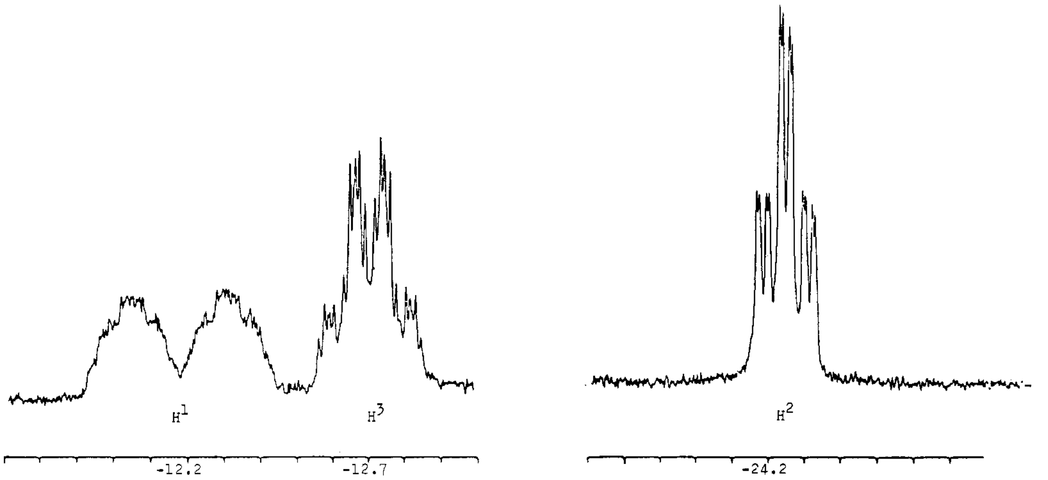

Figure 1. ^1H NMR spectrum of the compound $[(diphos)Rh(\mu\text{-}H)(\mu\text{-}Cl)IrH_2(PEt_3)_2]$ (**7a**).

Although the reaction mechanism for the formation of this dichloro-bridged compound is not known, we note that dichloro-bridged species are formed preferentially over their monochloro, monohydrido isomers when (1) the reaction time is increased, as is the case for the formation of **9**, or (2) a bulky phosphine is coordinated to the iridium atom; e.g., when PMe_2Ph is used, one obtains $[(diphos)Rh(\mu\text{-}H)(\mu\text{-}Cl)IrCl(PMe_2Ph)_3]^+$ (**1b**), while $PMePh_2$ gives $[(diphos)Rh(\mu\text{-}Cl)_2IrH(PMePh_2)_3]^+$ (**10**).[10]

The IR spectra of compounds **7**, **8a**, and **8b** show two bands at ca. 2200 and 2060 cm^{-1} assignable to the stretching vibrations of the terminal hydride ligands, H^2 and H^3. For compound **9** absorptions at 2250 (sh) cm^{-1} and at 2220 cm^{-1} were observed.

The presence of the hydride ligands in compounds **7**, **8**, and **9** is indicated by their ^1H NMR spectra (see Table I). Thus compound **7** shows three sets of signals centered at −12.2, −12.7, and −24.2 ppm of relative intensities 1:1:1, assigned to H^1, H^3, and H^2, respectively. The assignment of the signals due to H^1 is based on the magnitude of $^2J(P^4,H)$[15] while the signals due to H^2 and H^3 were assigned on the basis of the observation that in related binuclear hydrido-bridged complexes the values of $^2J(H,H_{cis})$ are larger than those of $^2J(H,H_{trans})$.[10] Using these empirical observations and selective phosphorus decoupling experiments, it was possible to assign all the coupling constants between the hydride ligands and the phosphorus atoms for compound **7**. A simulated spectrum of the hydride region using these parameters is in good agreement with the experimental spectrum shown in Figure 1. The hydride ligands of compound **9** give rise to a triplet at −28.4 ppm.

The $^{31}P\{^1H\}$ NMR spectra of compounds **7** and **8** (see Table II) show three sets of signals: two of them appear at lower fields, each as a doublet of doublets, assigned to P^3, and a set of four triplets, assigned to P^4. The assignment of the low-field signals to P^3 and P^4 was made on the basis of an off-resonance spectrum (which showed only a broadening of the set of four triplets) and the assumption that $^2J(P,H_{trans}) > {}^2J(P,H_{cis})$. The equivalent P^1 and P^2 donor atoms give a doublet at higher field. The long-range couplings between P^1, P^2, and P^4 provide additional support for the binuclear formulation of compounds **7** and **8**. The complex $[(diphos)Rh(\mu\text{-}Cl)_2IrH_2(P\text{-}i\text{-}Pr_3)_2]$ (**9**) showed a doublet at 75.9 ppm for the phosphorus atoms on rhodium, P^3 and P^4, and a singlet at 33.4 ppm for those on iridium, P^1 and P^2.

^{31}P and ^1H NMR spectroscopic studies show that compound **8a** readily reacts with CO, giving the mononuclear complexes *trans*-$[RhCl(CO)(PEt_3)_2]$,[16] *mer-trans*-$[IrH_3(CO)(PEt_3)_2]$,[17] and other unidentified iridium species.

However, as noted elsewhere,[10] the binuclear complex $[(diphos)Rh(\mu\text{-}H)(\mu\text{-}Cl)IrH(PEt_3)_3]BF_4$ (**2**) is cleaved by CO, giving $[Rh(CO)_3(diphos)]BF_4$ and *mer-trans*-$[IrHCl_2(PEt_3)_3]$. Thus, in this case, no CO-containing iridium complex is formed.

Compound **7** catalyzes the hydrogen of olefins, e.g. of 1-hexene to hexane, but the reaction rates are slower than those with the

---

(15) Pregosin, P. S.; Kunz, R. W. In "NMR Principles and Progress"; Springer-Verlag: New York: 1979; Vol. 16.

(16) Garrou, P. F.; Hartwell, S. E. *Inorg. Chem.* **1976**, *15*, 646.

(17) This structural assignment was based on its NMR parameters. The ^{31}P NMR spectrum showed a singlet at 0.36 ppm, which, when observed under "off-resonance" conditions, appeared as a quartet. The ^1H NMR spectrum showed two signals at −8.15 and −11.2 ppm with relative intensities 2:1. The first signal is a doublet of triplets ($^2J(P,H) = 19$ Hz and $^2J(H,H) = 4.9$ Hz). The latter signal, which should appear as a triplet of triplets, is insufficiently resolved to observe this splitting. The related compound *mer-trans*-$[IrH_3(CO)(PEt_3Ph)_2]$ has been reported by: Mann, B. E.; Masters, C.; Shaw, B. L. *J. Chem. Soc. D* **1970**, 846.

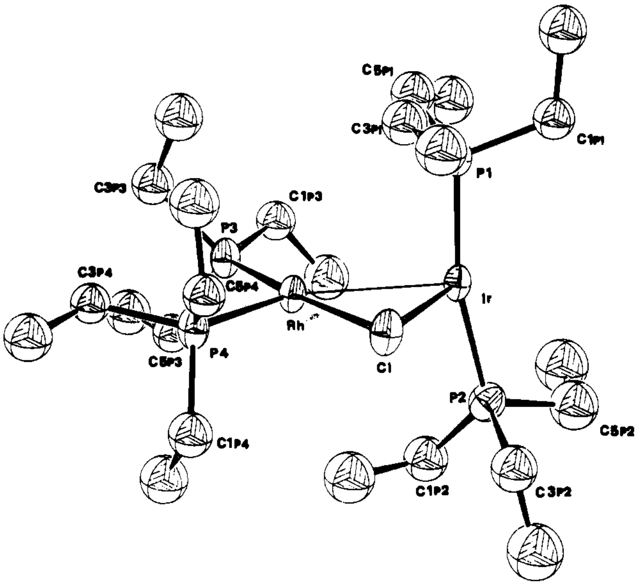

Figure 2. ORTEP drawing of the molecular structure of $[(PEt_3)_2Rh(\mu\text{-}H)(\mu\text{-}Cl)IrH_2(PEt_3)_2]$ (**8a**).

cation $[Rh(diphos)(solvent)_2]^{+}$,[18] and thus these experiments were not pursued further.

Attempts were made to obtain a trinuclear hydrido-bridged complex from **8a** and $[Rh(diphos)(ac)_2]BF_4$ (ac = acetone):

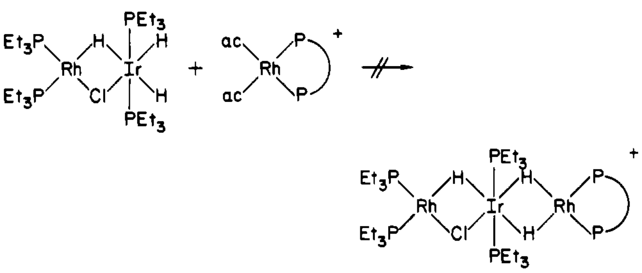

However, we obtained compound **7** and a complex containing a "$Rh(PEt_3)_2$" moiety as shown by ^1H and ^{31}P NMR spectroscopy. Probably a short-lived trinuclear species, **11**, was formed, which rearranged to the thermodynamically more stable product **7**.

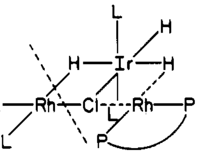

11, L = PEt_3

X-ray Crystal Structure of $[(PEt_3)_2Rh(\mu\text{-}H)(\mu\text{-}Cl)IrH_2(PEt_3)_2]$ (8a). The structure consists of discrete molecules held together by van der Waals forces with no unusual packing interactions.

Compound **8a** may be described as formed by a square-planar Rh(I) unit having as ligands the two P atoms of PEt_3 and the bridging chloride and hydride atoms. The last two ligands complete an octahedral *mer*-$[IrH_2Cl(PEt_3)_2]$ unit. Both coordination polyhedra are distorted (cf. Table III and Figure 2).

Even though it proved impossible to locate the hydrogen atoms (both bridging and terminal), their positions are unequivocally defined by the crystal coordination geometry and the NMR data (see above).

The geometry of compound **8a** is best discussed by comparing it with the structures of the related complexes, both mono- and binuclear, given in Table IV.

The metal–metal distance, in this compound (2.899 (1) Å), is shorter than that in $[(diphos)Rh(\mu\text{-}H)(\mu\text{-}Cl)IrH(PEt_3)_3]^{+}$[10] (**2**) (2.969 (1) Å) and in $[(diphos)Rh(\mu\text{-}H)(\mu\text{-}Cl)IrCl(PEt_3)_3]^{+}$[10] (**1a**) (2.904 (1) Å). However, this separation in **8a** is longer than that in the dihydrido-bridged complex $[(diphos)Rh(\mu\text{-}H)_2IrH_2(P\text{-}i\text{-}Pr_3)_2]$[19] (**10**) (2.662 (1) Å).

Table III. Relevant Interatomic Distances (Å), Bond Angles (deg), and Torsion Angles (deg) for Compound 8a[b]

	Bond Distances		
Ir-Rh	2.898 (1)	P2-C1P2	1.86 (2)
Ir-Cl	2.496 (3)	P2-C3P2	1.81 (2)
Ir-P1	2.265 (4)	P2-C5P2	1.87 (2)
Ir-P2	2.274 (4)	P3-C1P3	1.84 (2)
Rh-Cl	2.429 (3)	P3-C3P3	1.84 (1)
Rh-P3	2.199 (4)	P3-C5P3	1.86 (2)
Rh-P4	2.245 (4)	P4-C1P4	1.84 (2)
P1-C1P1	1.86 (2)	P4-C3P4	1.86 (2)
P1-C3P1	1.82 (2)	P4-C5P4	1.85 (2)
P1-C5P1	1.85 (2)	$\langle C\text{-}C\rangle_{av}$[a]	1.54 (2)
	Bond Angles		
Ir-Cl-Rh	72.10 (9)	Ir-P1-C5P1	119.84 (42)
Ir-Rh-P3	116.99 (8)	Ir-P2-C1P2	113.27 (55)
Ir-Rh-P4	145.11 (6)	Ir-P2-C3P2	123.60 (42)
Rh-Ir-P1	91.74 (10)	Ir-P2-C5P2	111.44 (52)
Rh-Ir-P2	101.77 (10)	Rh-P3-C1P3	117.81 (42)
P1-Ir-P2	166.39 (13)	Rh-P3-C3P3	114.55 (43)
P3-Rh-P4	97.90 (14)	Rh-P3-C5P3	119.42 (43)
Cl-Ir-P1	97.05 (13)	Rh-P4-C1P4	111.86 (49)
Cl-Ir-P2	92.9 (13)	Rh-P4-C3P4	124.65 (38)
Cl-Rh-P3	171.96 (12)	Rh-P4-C5P4	113.80 (44)
Cl-Rh-P4	90.09 (13)	$\langle P\text{-}C\text{-}C\rangle$[a]	114 (2)
Ir-P1-C1P1	115.73 (47)	$\langle C\text{-}P\text{-}C\rangle$[a]	101 (2)
Ir-P1-C3P1	112.28 (46)		
	Torsion Angles		
Ir-Cl-Rh-P3	−179.4 (5)	P1-Ir-Rh-P3	83.6 (7)
Ir-Cl-Rh-P4	1.0 (5)	P1-Ir-Rh-P4	−96.4 (5)
P1-Ir-Cl-Rh	−102.9 (6)	P2-Ir-Rh-P3	−94.7 (5)
P2-Ir-Cl-Rh	86.8 (6)		

[a] Average values. The esd on averaged distances was obtained by using the formula $d_{av} = [\Sigma(d_i - \overline{d})^2/(N-1)]^{1/2}$ giving the scatter from the average value. [b] Esd's on the last significant digit are given in parentheses.

The short Rh–Ir distance in compound **10** must be taken to imply that there is a significant metal–metal interaction. A comparable M–M interaction can be assumed also for the isolobal compound $[(PEt_3)_2Pt(\mu\text{-}H)_2IrH_2(PEt_3)_2]^{+}$[20] (**11**) (Pt–Ir = 2.676 (1) Å and the sum of the atomic radii equals 2.744 Å).[25] On the other hand, the longer Rh–Ir distance in compound **8a**, which is in the upper range of distances at which such interactions are postulated,[9] is indicative of a weaker metal–metal interaction than in compound **10**.

It should be noted that the replacement of one of the hydrides, in a dihydrido-bridged unit, by another donor atom is accompanied by a lengthening of the M–M distance.[9,26]

The shorter Rh–Ir separation in compound **8a** relative to that in **2** and **1a** may arise from the presence of a positive charge on compounds **2** and **1a** while **8a** is uncharged: it is known that positive charges on transition-metal complexes cause contraction of electron density.[27]

---

(18) Halpern, J.; Riley, D. P.; Chan, A. S. C.; Pluth, J. J. *J. Am. Chem. Soc.* **1977**, *99*, 8055.

(19) Musco, A.; Naegeli, R.; Venanzi, L. M.; Albinati, A. *J. Organomet. Chem.* **1982**, *228*, C15.

(20) Emge, T. J.; Koetzle, T. F.; Albinati, A.; Venanzi, L. M. American Crystallographic Association Meeting Abstracts, Columbia, MO, 1983.

(21) Bau, R.; Carroll, W.; Hart, D. W.; Teller, R. G.; Koetzle, T. F. "Transition Metal Hydrides"; Bau, R., Ed.; American Chemical Society: Washington, DC, 1978, *Adv. Chem. Ser.* No. 167, p 73.

(22) Clark, S. R.; Skelton, B. W.; Waters, T. N. *Inorg. Chim. Acta* **1975**, *12*, 235.

(23) Robertson, G. B.; Tucker, P. A. *J. Am. Chem. Soc.* **1982**, *104*, 317.

(24) Lehner, H.; Matt, D.; Pregosin, P. S.; Venanzi, L. M.; Albinati, A. *J. Am. Chem. Soc.* **1983**, *104*, 1825.

(25) Donhue, J. In "The Structure of the Elements"; Wiley: New York, 1974; pp 215–219.

(26) Jans, J.; Naegeli, R.; Venanzi, L. M.; Albinati, A. *J. Organomet. Chem.* **1983**, *247*, C37.

(27) Kauzmann, W. In "Quantum Chemistry"; Academic Press: New York, 1957.

Table IV. Some Bond Lengths (Å) and Angles (deg) for Mono- and Binuclear Iridium-Containing Complexes[h]

compd	Rh-Cl-Ir	Ir-P(ax)	Ir-P(eq, trans H)	M-(μ-Cl)	M-Cl(term)	M-(μ-H)	Ir-H(term)	M-P	M-Ir
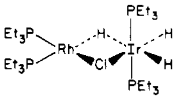 **8a**	72.10 (9)	2.263 (4) 2.272 (4)		2.494 (3)[a] 2.427 (3)[b]				2.245 (3)[b,c] 2.199 (3)[b]	2.899 (1)
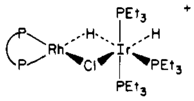 **2**[10]	74.5 (1)	2.369 (6) 2.362 (6)	2.245 (7)	2.510 (5)[a] 2.394 (5)[b]				2.215 (6)[b,c] 2.213 (6)	2.969 (2)
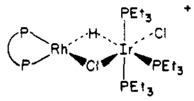 **1a**[10]	75.05 (7)	2.390 (3) 2.384 (3)	2.367 (3)	2.386 (3)[b] 2.381 (3)[a]	2.366 (3)	1.85 (8)[b] 1.67 (8)[a]		2.216 (3)[a] 2.199 (3)	2.904 (1)
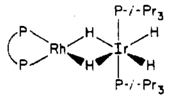 **10**[19]		2.293 (2)						2.197 (2)	2.662 (1)
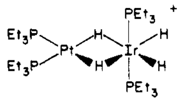 **11**[20]		2.300 (2) 2.299 (2)				1.882 (3)[a] 1.880 (3)[a] 1.736 (3)[d] 1.726 (3)[d]	1.591 (3) 1.586 (3)	2.276 (2)[d]	2.677 (1)
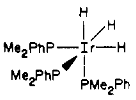 **12**[21]		2.296 (3) (⟨Ir–P⟩$_{av}$)							
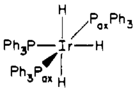 **13**[22]		2.287 (3) 2.285 (3)	2.347 (3)						
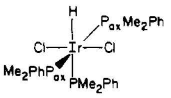 **14**[23]		2.329 (2)	2.365 (2)		2.364 (2) 2.402 (2)		1.616 (7)		
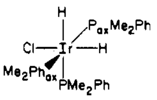 **15**[23]		2.292 (2)	2.331 (2)		2.505 (1)		1.603 (8) 1.557 (9)		
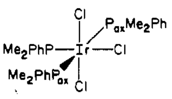 **16**[23]		2.381 (2) 2.366 (2) 2.280 (2)[f]			2.437 (2)[g] 2.366 (1)				
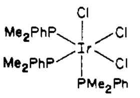 **17**[23]		2.289 (2)			2.463 (2)				
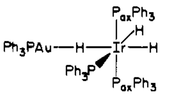 **18**[24]		2.334 (6) 2.325 (6)	2.397 (4)						2.765 (1)

[a] M = Ir. [b] M = Rh. [c] P trans to H. [d] M = Pt. [e] H trans to P. [f] P trans to Cl. [g] Cl trans to P. [h] Key: ax = axial; eq = equatorial; term = terminal.

As expected from the shorter Rh–Ir distance in **8a** than in **2** and **1a**, the Rh–Cl–Ir bond angle in **8a** (72.10 (9)°) is smaller than those in **2** and **1a** (74.5 (1) and 75.05 (7)°, respectively). Similarly, in the compounds [(η^5-C_5Me_5)ClM(μ-H)(μ-Cl)MCl(η^5-C_5Me_5)] (M = Rh, Ir)[9] M–M distances of ca. 2.90 Å occur with M–Cl–M angles of ca. 73° (μ-H, μ-Cl) while M–M distances of ca. 3.73 Å are associated with M–Cl–M angles of ca. 99°.

The following structural features are also worthy of note:

(1) It is observed that the Ir–Cl distance in complexes **1a**, **2**, **8a**, and **10–18** is long (from 2.49 to 2.51 Å) when the trans ligand

is a hydride and short (from 2.38 to 2.40 Å) when the trans ligand is a chloride. This is a typical trans-influence behavior.[28]

(2) Replacement of a chloride by a hydride ligand in the complexes listed in Table IV, in addition to the effect mentioned under (1), causes a *shortening* of the Ir–P bonds in cis positions. Thus the Ir–P distance in compound **14** is 2.329 (2) Å while that in compound **15** is 2.292 (2) Å. This effect is observed also in the binuclear complexes **2** and **1a**; e.g., the Ir–P$_{\mathrm{ax}}$ and Ir–P$_{\mathrm{eq}}$ distances in **2** are ⟨2.365 (2)⟩ and 2.245 (7) Å, respectively, while the Ir–P$_{\mathrm{ax}}$ and Ir–P$_{\mathrm{eq}}$ distances in **1a** are ⟨2.387 (3)⟩ and 2.367 (3) Å, respectively.

(3) Attaching a second metal center (with its own ligands) to a hydride with formation of an M–H–M′ bridge results in a lengthening of the M–P bonds. Thus the Ir–P$_{\mathrm{ax}}$ and Ir–P$_{\mathrm{eq}}$ distances in compound **13** are ⟨2.286 (3)⟩ and 2.347 (3) Å, respectively, while the corresponding distances in compound **18** are ⟨2.329 (6)⟩ and 2.397 (4) Å, respectively. This effect has been commented on elsewhere.[24]

(4) The Ir–(μ-Cl) bond distance is longer in **2** than in **1a** presumably because of the effect (1) mentioned above. As the Rh–Cl–Ir bond angles in compounds **2** and **1a** are almost identical, the Ir–Cl bond lengthening results in a longer Rh–Ir distance in the former compound.

(5) The Ir–Cl bond length in **8a** is slightly shorter than in **2**. This difference may be a result of a stronger M–M interaction, which results in a shorter M–M distance and a smaller M–Cl–M bond angle, a sort of compression effect.

(6) While there is an overall lengthening of Ir–P$_{\mathrm{eq}}$ bonds on hydrido-bridge formation, its effect on Ir–P$_{\mathrm{eq}}$ bonds requires further comment. If one considers the corresponding bond lengths in the mononuclear complexes as a reference point, one finds that in the binuclear complexes the Ir–P$_{\mathrm{eq}}$ distance becomes longer when the ligand in the position cis to Ir–P$_{\mathrm{eq}}$ is chloride and shorter when it is hydride. This observation may be related to the operation of a strong cis influence.[29]

(7) As expected, the Rh–P distances are equal in the symmetrical complexes **10** and **11**. For the unsymmetrical complexes **8a**, **2**, and **1a** their lengths appear to be related to the extent of the Rh–Ir interaction: where the interaction is stronger, e.g., in **1a**, they differ significantly, the long bond being that in the position trans to the H ligand, while the two bonds are practically equal in **2**, which shows the longest Rh–Ir bond.

(8) The preference for the formation of a Rh(μ-H)(μ-Cl)Ir arrangement over Rh(μ-H)$_2$Ir is likely to be due to electron availability for bridge building: in the case of μ-H it leads to the formation of a three-center–two-electron system while a chloride bridge can result, at least potentially, in a three-center–four-electron interaction. The preference for (μ-Cl)$_2$ over (μ-H)(μ-Cl) has also been observed, i.e., in the formation of compound **9**, but as mentioned earlier, it appears to be associated with steric repulsions.

Experimental Section

All operations were carried out under purified nitrogen. Solvents were distilled under nitrogen and dried prior to use. Elemental analyses were performed by the Microanalytical Laboratory of the Swiss Federal Institute of Technology (ETH). Infrared spectra in the region 400-4000 cm^{-1} were recorded on a Beckman IR 4250 spectrophotometer as KBr pellets or Nujol mulls. The ^{1}H NMR spectra were recorded at 90 and/or 250 MHz, respectively, on an FT Bruker WH-90 or 250 spectrometer. The ^{31}P{^{1}H} NMR spectra were measured with use of the WH-90 spectrometer. ^{1}H and ^{31}P chemical shifts are given relative to Me$_4$Si and H$_3$PO$_4$, respectively. A positive sign denotes a shift downfield of the reference.

A. Syntheses. [Rh$_2$Cl$_2$(C$_2$H$_4$)$_4$],[11] [RhCl(C$_2$H$_4$)(diphos)],[12] [Rh$_2$Cl$_2$(diphos)$_2$],[12] [Rh((CH$_3$)$_2$CO)$_2$(diphos)][BF$_4$],[18] [IrH$_5$(PEt$_3$)$_2$],[14] and [IrH$_2$(P-*i*-Pr$_3$)$_2$][15] were prepared as described in the appropriate references.

Table V. Crystal Data and Data Collection Parameters for Compound 8a

formula	$C_{24}H_{63}ClIrP_4Rh$
fw	806.22
a, Å	11.507 (2)
b, Å	15.974 (4)
c, Å	19.198 (4)
β, deg	103.19 (4)
V, Å^3	3434.7 (3)
Z	4
ρ_{calcd}, g cm^{-3}	1.56
space group	$P2_1/c$
cryst dimens, mm	0.25 × 0.40 × 0.30
radiation	Mo K$\bar{\alpha}$ (graphite monochromated, $\lambda = 0.71069$ Å)
μ, cm^{-1}	45.97
θ range, deg	$2.5 \leqslant \theta \leqslant 24.0$
scan mode	$\omega/2\theta$
scan speed, deg s^{-1}	0.04
scan width, deg	1.20
total bkgd time, s	20
receiving apertures, deg	1.0 (horiz), 1.0 (vert)
no. of data collected	4946 ($\pm h,+k,+l$)
no. of obsd data ($I \geqslant 3\sigma(I)$)	3806
$R = \Sigma \lvert\Delta F\rvert / \Sigma \lvert F_o\rvert$ [a]	0.059
$R_w = (\Sigma \lvert\Delta F\rvert / \Sigma w \lvert F_o\rvert^2)^{1/2}$	0.063

[a] For the observed reflections.

[(PEt$_3$)$_2$Rh(μ-H)(μ-Cl)IrH$_2$(PEt$_3$)$_2$] (8a). PEt$_3$ (0.118 g, 1 mmol) was added dropwise to a well-stirred solution of [Rh$_2$Cl$_2$(C$_2$H$_4$)$_4$] (0.097 g, 0.25 mmol) in toluene (10 mL). After slow addition of [IrH$_5$(PEt$_3$)$_2$] (0.217 g, 0.5 mmol) dissolved in toluene (10 mL) and heating until the reaction mixture had become red-brown, the solution was stirred for 2.5 h at room temperature. The solvent was then evaporated under reduced pressure, and the residue was now dissolved in ca. 10 mL of methanol. Orange needles of **8a** were obtained on cooling the solution (0.31 g, 77%). Anal. Calcd for C$_{24}$H$_{63}$ClIrP$_4$Rh: C, 35.75; H, 7.82. Found: C, 35.54; H, 7.75. IR (Nujol): ν(Ir–H) 2180 (m), 2060 (m) cm^{-1}.

[(diphos)Rh(μ-H)(μ-Cl)IrH$_2$(PEt$_3$)$_2$] (7a). [Rh$_2$Cl$_2$(diphos)$_2$] (0.108 g, 9.1 mmol) was suspended in toluene (5 mL) and reacted with [IrH$_5$(PEt$_3$)$_2$] (0.139 g, 0.3 mmol) in toluene (5 mL). The mixture then was refluxed for 5 min, filtered, and concentrated. After addition of methanol and cooling at −20 °C, **7b** precipitated as orange crystals (0.080 g, 41%). Anal. Calcd for C$_{38}$H$_{57}$ClIrP$_4$Rh: C, 47.13; H, 5.89. Found: C, 46.50; H, 5.85. IR (Nujol): ν(Ir–H) 2210 (m), 2060 (m) cm^{-1}.

[(diphos)Rh(μ-H)(μ-Cl)IrH$_2$(P-*i*-Pr$_3$)$_2$] (7b). [Rh$_2$Cl$_2$(C$_2$H$_4$)$_4$] (0.049 g, 0.126 mmol) was dissolved in benzene (10 mL) and reacted with a solution of diphos (0.100 g, 0.25 mmol) in benzene (20 mL). Then a solution of [IrH$_5$(p-*i*-Pr$_3$)$_2$] (0.130 g, 0.25 mmol) in benzene (20 mL) was added under hydrogen and refluxed for 0.5 h. After filtration, addition of methanol, and cooling at −20 °C, **7b** precipitated as orange crystals (0.040 g, 15%). This product was always contaminated with some **9**. IR (Nujol): ν(Ir–H) 2210 (m), 2060 (m) cm^{-1}.

[(diphos)Rh(μ-Cl)$_2$IrH$_2$(P-*i*-Pr$_3$)$_2$] (9). [Rh$_2$L$_2$(C$_2$H$_4$)$_4$] (0.049 g, 0.126 mmol) in benzene (10 mL) was reacted with a solution of diphos (0.100 g, 0.25 mmol) in benzene (20 mL). Then [IrH$_5$(p-*i*-Pr$_3$)$_2$] (0.130 g, 0.25 mmol) dissolved in benzene (5 mL) was added and the reaction mixture was refluxed for 1 h. After concentration, filtration, and cooling at −20 °C, dark crystals of **9** were obtained (0.050 g, 18%). Some crystals of **5** could also be identified. Anal. Calcd for C$_{44}$H$_{68}$Cl$_2$IrP$_4$Rh: C, 48.61; H, 6.26. Found: C, 48.79; H, 6.30. IR (Nujol): ν(Ir–H) 2250 (sh), 2220 (m) cm^{-1}.

Reaction of 8a with [(diphos)Rh(ac)$_2$]BF$_4$. Complex **8a** (0.100 g, 0.10 mmol) in acetone (20 mL) was reacted with an acetone solution of [(diphos)Rh(ac)$_2$]BF$_4$ (0.072 g, 0.10 mmol; ac = acetone). The reaction mixture turned red-brown immediately. The ^{31}P NMR spectrum of a solution obtained by evaporating the solvent and dissolving the residue in CDCl$_3$ unambiguously revealed the presence of a "Rh(PEt$_3$)$_2$" moiety (δ 73.5, d, ^2J(Rh,P) = 176 Hz). The solid obtained by adding Et$_2$O to the solution was dried under vacuum. A ^{1}H NMR measurement on the residual solid confirmed the presence of **7a**.

Catalytic Hydrogenation Experiment Using 7a. A solution of **7a** (0.051 g, 0.053 mmol), in CH$_2$Cl$_2$ (50 mL), and 1-hexene (2.0 g, 23.8 mmol) were placed in a steel autoclave. The mixture was stirred for 8 h under an H$_2$ pressure of 5 atm. The analysis of the reaction mixture showed a hexane conversion of 25%.

Reaction of 7a with CO. CO was bubbled for a few minutes through a solution of **7a** (0.060 g) in benzene-d_6 (3 mL). The solution immediately became paler. Its ^{31}P NMR spectrum showed the presence of

---

(28) Burdett, J. K. In "Molecular Shapes"; Wiley: New York, 1980; Chapter 12.

(29) Pidcock, A. In "Catalytic Aspects of Metal Phosphine Complexes"; Alyez, E. C., Meek, D. W., Eds.; American Chemical Society: Washington, DC, 1982; *Adv. Chem. Ser.* No. 196, p 1, and references quoted therein.

Table VI. Positional Parameters for the Compound $[(PEt_3)_2Rh(\mu\text{-}H)(\mu\text{-}Cl)IrH_2(PEt_3)_2]$ (8a)[a]

	x/a	y/b	z/c
Ir	0.17117 (4)	0.13785 (3)	0.26804 (3)
Rh	0.36331 (8)	0.25922 (6)	0.28996 (6)
P1	0.11612 (31)	0.16857 (23)	0.14991 (20)
P2	0.18646 (34)	0.08826 (26)	0.38080 (22)
P3	0.31666 (30)	0.39010 (21)	0.30628 (20)
P4	0.55933 (29)	0.27793 (22)	0.29819 (21)
Cl	0.38623 (29)	0.11006 (20)	0.27265 (20)
C1P1	0.0456 (15)	0.2728 (11)	0.1274 (9)
C2P1	−0.0669 (17)	0.2870 (12)	0.1561 (10)
C3P1	0.0041 (14)	0.0960 (10)	0.1012 (9)
C4P1	−0.0453 (17)	0.1119 (12)	0.0211 (10)
C5P1	0.2302 (15)	0.1726 (11)	0.0957 (9)
C6P1	0.2866 (17)	0.0880 (13)	0.0873 (11)
C1P2	0.0445 (17)	0.0440 (13)	0.3953 (11)
C2P2	−0.0497 (21)	0.1153 (15)	0.3956 (13)
C3P2	0.2329 (16)	0.1518 (11)	0.4606 (9)
C4P2	0.3627 (19)	0.1853 (14)	0.4690 (11)
C5P2	0.2842 (16)	−0.0064 (12)	0.3983 (9)
C6P2	0.3021 (21)	−0.0449 (16)	0.4733 (13)
C1P3	0.1582 (14)	0.4151 (10)	0.3001 (9)
C2P3	0.1062 (17)	0.3729 (12)	0.3592 (10)
C3P3	0.3861 (14)	0.4329 (10)	0.3957 (8)
C4P3	0.3535 (16)	0.5241 (12)	0.4113 (10)
C5P3	0.3508 (15)	0.4727 (11)	0.2455 (9)
C6P3	0.3215 (16)	0.4459 (12)	0.1670 (10)
C1P4	0.6506 (15)	0.2286 (11)	0.3792 (9)
C2P4	0.6458 (16)	0.2760 (12)	0.4492 (10)
C3P4	0.6324 (15)	0.3814 (10)	0.2966 (9)
C4P4	0.7674 (16)	0.3813 (12)	0.3085 (10)
C5P4	0.6177 (14)	0.2193 (10)	0.2305 (8)
C6P4	0.5736 (16)	0.2560 (13)	0.1540 (10)

[a] Esd's on the last significant digit are given in parentheses.

trans-$[RhCl(CO)(PEt_3)_2]$ (δ −23.5, d, ${}^2J(Rh,P) = 178$ Hz) and *mer-trans*-$[IrH_3(CO)(PEt_3)_2]$ (${}^1H$ NMR δ −11.2 (complex m, H trans to CO), δ −8.15 (dt, H trans to H, ${}^2J(P,H) = 19$ Hz, ${}^2J(H,H) = 4.9$ Hz),${}^{31}P\{{}^1H\}$ NMR 0.4 ppm (s)). Other unidentified products were also present. Attempts to fully characterize these were unsuccessful.

B. Determination and Refinement of the Structure. Orange crystals of $[(PEt_3)_2Rh(\mu\text{-}H)(\mu\text{-}Cl)IrH_2(PEt_3)_2]$ (**8a**) were obtained by slow evaporation from methanol and are air stable. A suitable crystal of irregular prismatic habit was chosen for the data collection and mounted, at random orientation, on a glass fiber.

Crystal data are listed in Table V. The determination of the lattice parameters and space group and the data collection were carried out, at room temperature, on a Philips PW 1100 automated four-circle diffractometer. The systematic absences ($0k0$, $k = 2n$; $h0l$, $l = 2n$) allowed the unambiguous assignment of the $P2_1/c$ space group. The cell parameters were obtained by least-squares fit of the 2θ values of 20 accurately centered, high-order reflections ($16.0 \leq 2\theta \leq 30°$).

Three standard reflections, 1,−1,−2, 1,1,−2, and −1,−1,2, were measured every 2 h to check the stability and the orientation of the crystal. No significant variations in the diffracted intensities were detected during data collection. An empirical absorption correction was applied with use of an azimuthal (ψ) scan of three reflections (040, 060, 080) at high χ angles (85.70°); transmission factors were in the range 0.69–0.92.

Data were corrected for Lorentz and polarization factors.[30] The standard deviations on the intensities were calculated in terms of statistics alone, considering as observed the reflections having $I_{net} \geq 3\sigma(I)$.

The structure was solved by standard Patterson and Fourier methods and refined by block-diagonal least squares using a Cruickshank[31] weighting scheme; the function minimized was $[\sum w(|F_o| - (1/k)|F_c|)^2]$. Anisotropic temperature factors for Rh, Ir, P, and Cl atoms and isotropic factors for carbon atoms were used.

The hydrogens of the carbon atoms were placed in idealized positions, assuming a C–H bond length of 1.00 Å, and were assigned individual isotropic temperature factors, $B = 6.50$ Å^2. Their contribution was taken into account but not refined. No extinction correction was found to be necessary.

Scattering factors were taken from ref[32], and the contribution of the real part of the anomalous dispersion was taken into account for Rh, Ir, Cl, and P atoms. Upon convergence (no shifts greater than 0.4σ) the final conventional agreement factor was 0.059 (see Table V). A final difference Fourier map showed no anomalous features, and no significant peaks in the hydride regions were detected.

All the calculations were performed on a Univac 1100 using local verson of data reduction, structure factor, Fourier, and least-squares programs.[33] The drawing was made with use of the ORTEP[34] program with thermal ellipsoids drawn at 50% probability. The final positional parameters are given in Table VI.

Acknowledgment. H.L. received support from the Swiss National Science Foundation. We are greatly indebted to Dr. P. S. Pregosin for much valuable discussion and to I. Fecker for some experimental assistance with this work. A.A. was partly supported by a CNR Grant.

Supplementary Material Available: Tables containing calculated hydrogen positions (Table A), thermal factors (Table B), and observed structure factors (Table C) (33 pages). Ordering information is given on any current masthead page.

---

(30) Arndt, U. V.; Willis, B. T. M. "Single Crystal Diffractometry"; Cambridge University Press: New York, 1966; p 286.

(31) Cruickshank, D. W. J. In "Computing Methods in Crystallography"; Ahmed, A., Ed.; Munksgaard: Copenhagen.

(32) "International Tables for X-ray Crystallography"; Kynoch Press: Birmingham, England, 1974; Vol. IV.

(33) Albinati, A.; Brückner, S. *Acta Crystallogr., Sect. B: Struct. Crystallogr. Cryst. Chem.* **1978**, *B34*, 3390 and references quoted therein.

(34) Johnson, C. K. *Oak Ridge Natl. Lab., [Rep.] ORNL (U.S.)* **1965**, *ORNL-3794*.